



# Population Pharmacokinetic Model of *N*-acetylmannosamine (ManNAc) and *N*-acetylneuraminic acid (Neu5Ac) in Subjects with GNE Myopathy

Scott Van Wart<sup>1</sup> · Donald E. Mager<sup>1</sup> · Cindy J. Bednasz<sup>1</sup> · Marjan Huizing<sup>2</sup> · Nuria Carrillo<sup>2</sup>

Accepted: 10 March 2021 / Published online: 24 April 2021  
© The Author(s) 2021

## Abstract

**Background** GNE myopathy is a rare genetic muscle disease resulting from deficiency in an enzyme critical for the biosynthesis of *N*-acetylneuraminic acid (Neu5Ac, sialic acid). The uncharged Neu5Ac precursor, *N*-acetylmannosamine (ManNAc), is under development as an orphan drug for treating GNE myopathy.

**Methods** A semi-mechanistic population pharmacokinetic model was developed to simultaneously characterize plasma ManNAc and its metabolite Neu5Ac following oral administration of ManNAc to subjects with GNE myopathy. Plasma ManNAc and Neu5Ac pharmacokinetic data were obtained from two clinical studies (ClinicalTrials.gov identifiers NCT01634750, NCT02346461) and were simultaneously modeled using NONMEM.

**Results** ManNAc and Neu5Ac plasma concentrations were obtained from 34 subjects with GNE myopathy (16 male, 18 female, median age 39.5 years). The model parameter estimates included oral absorption rate ( $k_a$ ) = 0.256 h<sup>-1</sup>, relative bioavailability relationship with dose ( $F$ -Dose) slope = -0.405 (where  $F = 1$  for 6-g dose), apparent clearance ( $CL_M/F$ ) = 631 L/h, volume of distribution ( $V_M/F$ ) = 506 L, Neu5Ac elimination rate constant ( $k_{out}$ ) = 0.283 h<sup>-1</sup>, initial ManNAc to Neu5Ac conversion ( $SLP_0$ ) = 0.000619 (ng/mL)<sup>-1</sup> and at steady-state ( $SLP_{SS}$ ) = 0.00334 (ng/mL)<sup>-1</sup>, with a rate-constant of increase ( $k_{inc}$ ) = 0.0287 h<sup>-1</sup>. Goodness-of-fit plots demonstrated an acceptable and unbiased fit to the plasma ManNAc and Neu5Ac concentration data. Visual predictive checks demonstrated reasonable agreement between the 5th, 50th, and 95th percentiles of the observed and simulated data.

**Conclusions** This population pharmacokinetic model can be used to evaluate ManNAc dosing regimens and to calculate Neu5Ac production and exposure following oral administration of ManNAc in subjects with GNE myopathy.

## 1 Introduction

GNE myopathy (OMIM 605820) is a rare genetic muscle disease characterized by progressive muscle weakness and atrophy with onset in early adulthood [1, 2]. It is caused by biallelic pathogenic variants in the *GNE* gene, encoding the bifunctional enzyme UDP-*N*-acetylglucosamine (GlcNAc) 2-epimerase (EC:3.2.1.183)/*N*-acetylmannosamine (ManNAc) kinase (EC:2.7.1.60) (GNE), which catalyzes

### Key Points

This paper describes pharmacometric research of ManNAc administration in patients with GNE myopathy, a rare genetic muscle disease.

The population pharmacokinetic model presented provides a useful tool in the clinical drug development of ManNAc to guide dose selection and understand the effects of oral ManNAc administration on Neu5Ac production and exposure.

✉ Scott Van Wart  
svanwart@ePD-LLC.com

<sup>1</sup> Enhanced Pharmacodynamics, LLC, 701 Ellicott Street, Buffalo, New York 14203, USA

<sup>2</sup> Human Biochemical Genetics Section, Medical Genetics Branch, National Human Genome Research Institute, National Institutes of Health, Bethesda, MD 20892, USA

the rate-limiting step and regulates the intracellular biosynthesis of *N*-acetylneuraminic acid (Neu5Ac) (Fig. 1) [3, 4]. Neu5Ac is the predominant mammalian form of sialic acid [5] that serves as the major terminal, negatively charged, building block to glycoproteins and glycolipids (glycans) and

can mediate or modulate a wide variety of physiological and pathological processes [4, 6]. GNE plays an important role in cell-surface sialylation, as the downstream product of the Neu5Ac biosynthesis pathway, CMP-Neu5Ac, is the sialic acid donor to nascent glycans in the Golgi complex (Fig. 1) [4]. Although the disease mechanism of GNE myopathy is not entirely understood, various sources of evidence suggest that GNE mutations (mostly missense) cause decreased GNE enzymatic activity leading to decreased Neu5Ac biosynthesis and subsequent hyposialylation (bound Neu5Ac) of muscle glycans [1, 7–10].

*N*-Acetylmannosamine (ManNAc) is an uncharged monosaccharide under development as an orphan drug for GNE myopathy [2, 11]. ManNAc is the first committed precursor in the Neu5Ac biosynthetic pathway (Fig. 1), and as the only neutral intermediate of this pathway, it enters cells either by

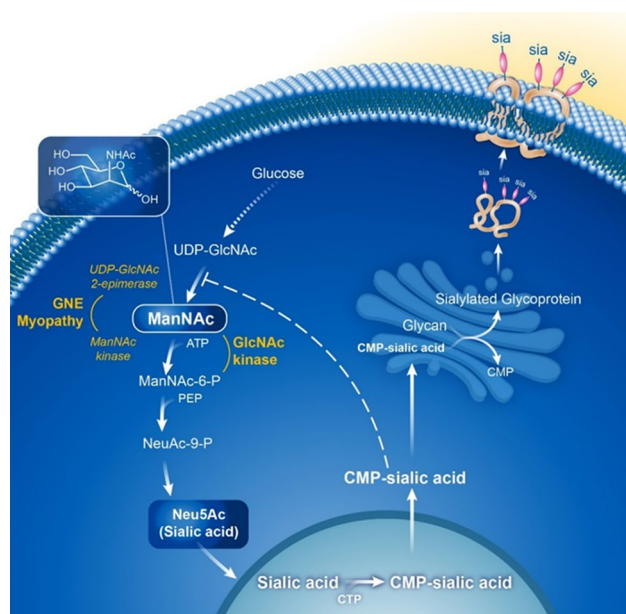


**Fig. 1** Neu5Ac (sialic acid) biosynthesis pathway. The first committed step of cytosolic Neu5Ac (sialic acid) biosynthesis is the conversion of UDP-GlcNAc to ManNAc by 2-epimerase activity of the bifunctional GNE enzyme, immediately followed by conversion of ManNAc to ManNAc-6-P by the kinase activity of the same GNE enzyme. ManNAc-6-P undergoes two more steps to form cytoplasmic free sialic acid. A nuclear step activates free sialic acid to CMP-sialic acid, which translocates back to the cytosol, where is utilized by the Golgi complex to sialylate glycans (glycoproteins and glycolipids). Cytoplasmic CMP-sialic acid also strongly feedback-inhibits the UDP-GlcNAc 2-epimerase enzymatic activity in its allosteric site (dashed line). Subjects with GNE myopathy have deficiency of GNE UDP-GlcNAc 2-epimerase and ManNAc kinase activity, resulting in decreased sialic acid production. Supplementation of ManNAc circumvents the feedback inhibition step in this pathway and increases sialic acid production. ManNAc can be converted to ManNAc-6-P by the ancillary enzyme GlcNAc kinase [24], which likely occurs in subjects with GNE myopathy with ManNAc kinase deficiency. *PEP* phosphoenolpyruvate. Figure reprinted from Xu et al. 2018 [11] with permission

passive diffusion or through a specific plasma-membrane transporter [12, 13]. The cellular uptake of ManNAc is linear and non-saturable up to 20 mM and is not influenced by the concentrations of glucose, serum, amino acids, vitamins, or glutamine in culture media [14]. ManNAc is situated in the sialic acid biosynthesis pathway after the rate-limiting reaction catalyzed by UDP-GlcNAc 2-epimerase, so its metabolism is not subject to feedback inhibition [4, 14, 15]. There is abundant experimental evidence that supplementation of ManNAc results in increased free Neu5Ac production and increased sialylation of glycans [4, 8, 16–18].

A first-in-human, randomized, placebo-controlled, double-blind pharmacokinetic phase I study of ManNAc in subjects with GNE myopathy (ClinicalTrials.gov identifier NCT01634750) showed that single doses of 3 g and 6 g were safe, but that doses of 10 g were associated with diarrhea and gastrointestinal tolerability issues [11]. Oral single doses of ManNAc were absorbed rapidly (time to maximum concentration [ $T_{max}$ ] 2–2.5 h) and caused significant and sustained increased plasma Neu5Ac concentrations ( $T_{max}$  8–11 h), which peaked approximately 6–8 hours after the  $T_{max}$  of ManNAc in subjects with GNE myopathy [11]. Given that Neu5Ac has a short half-life [18], the sustained increase in plasma Neu5Ac concentrations after a single ManNAc dose suggested that orally administered ManNAc is effective as a substrate for sustained intracellular Neu5Ac biosynthesis in subjects with GNE myopathy [11].

Here, we describe the development of a semi-mechanistic population pharmacokinetic model that simultaneously predicts the plasma concentrations of ManNAc and its metabolite, free Neu5Ac, which is not bound to glycans, following single and repeated oral dose administration to subjects with GNE myopathy. This semi-mechanistic model was developed as part of an iterative process that refined the model as data were accumulated. The model can be used to guide dose selection, evaluate the relative oral bioavailability of ManNAc, the conversion rate of ManNAc to Neu5Ac, and Neu5Ac exposure in subjects with GNE myopathy.

## 2 Methods

### 2.1 Subjects, Clinical Studies and Sample Collection

Subjects with GNE myopathy ( $N = 34$ ) were evaluated under NIH study 12-HG-0207 “Phase 1 Clinical Trial of ManNAc in Patients with GNE Myopathy” (ClinicalTrials.gov identifier NCT01634750), and NIH study 15-HG-0068 “An Open-Label Phase 2 Study of ManNAc in Subjects with GNE Myopathy” (ClinicalTrials.gov identifier NCT02346461); for additional study design details see Online Resource 1 in the electronic supplementary material (ESM). The protocols were approved by the National

Human Genome Research Institute (NHGRI) Institutional Review Board (IRB). All subjects gave written, informed consent and received ManNAc under FDA Investigational New Drug 078091. Plasma pharmacokinetic data for ManNAc and Neu5Ac from 34 subjects with GNE myopathy who participated in these studies were utilized in this analysis.

The estimated glomerular filtration rate (eGFR, in mL/min) was calculated using CKD-EPI cystatin C equation [19] since creatinine is not a reliable measure of kidney function in subjects with GNE myopathy, who typically have decreased muscle mass. In addition to the subjects' demographics, albumin and creatinine kinase were utilized as measures of hepatic injury, calculated eGFR was used as a measure of renal function, and other disease-related indices such as mutation type (epimerase/epimerase, epimerase/kinase, kinase/kinase, or deletion/kinase) were also explored to determine which patient covariate effects could explain a portion of the inter-individual variability in selected pharmacokinetic parameters.

## 2.2 Bioanalytical Assay for Plasma ManNAc and Neu5Ac Concentrations

The quantification of ManNAc and Neu5Ac in human plasma was performed by Alliance Pharma, Inc. (Malvern, PA, USA) using validated liquid chromatography and tandem mass spectrometry (LC-MS/MS) bioanalytical methods as previously described [20]; for additional details see Online Resource 2 (in the ESM).

## 2.3 Population Pharmacokinetic Model

### 2.3.1 Statistical Methods

Population analyses were performed to simultaneously analyze the plasma ManNAc and Neu5Ac concentration–time

data using NONMEM<sup>®</sup> Version 7.3 (ICON Development Solutions, Ellicott City, MD, USA) implementing the first-order conditional estimation method with  $\eta$ - $\epsilon$  interaction (FOCEI).

### 2.3.2 Pharmacokinetic Model Building

The population pharmacokinetic analyses was an iterative process conducted in stages based upon the availability of data (Table 1). In Stage 1, a structural population pharmacokinetic model was first developed using only the single-dose pharmacokinetic data for ManNAc and Neu5Ac from subjects with GNE myopathy in Study 12-HG-0207. Stage 2 consisted of updating the structural population pharmacokinetic model after including additional pharmacokinetic data for ManNAc and Neu5Ac from subjects with GNE myopathy receiving repeated doses of ManNAc in Study 15-HG-0068 (potential nonlinearity in Neu5Ac formation and adaptive feedback responses were explored). A formal covariate analysis was then performed to assess the potential of subject demographics, clinical laboratory variables, and disease-related indices to explain interindividual variability in ManNAc and Neu5Ac pharmacokinetic parameters. In Stage 3, simulations were conducted to support selection of a ManNAc dosing regimen that produces sustained increases in Neu5Ac concentrations upon repeated dosing in subjects with GNE myopathy. The population pharmacokinetic model was finalized in Stage 4 after including additional pharmacokinetic data for ManNAc and Neu5Ac from subjects with GNE myopathy receiving ManNAc at doses of 4 g three times daily (TID) during the last visit of Study 15-HG-0068. The population pharmacokinetic model parameter estimates in Table 4 are derived from this Final Population Pharmacokinetic Model.

Population pharmacokinetic models were minimally assessed via evaluation of individual and the population mean pharmacokinetic parameter estimates and their

**Table 1** Stages of population pharmacokinetic analysis

Stage of pharmacokinetic modeling	Data utilized	Modeling activities
Stage 1	ManNAc single dose pharmacokinetic data (Study 12-HG-0207)	Design of structural pharmacokinetic model Explore absorption models
Stage 2	ManNAc BID pharmacokinetic data (Study 15-HG-0068)	Covariate analysis Determination of non-linear and stationary pharmacokinetic
Stage 3	Stage 2 population pharmacokinetic model for ManNAc and Neu5Ac	Monte Carlo simulations of dosing regimens Recommendation for evaluation of additional TID dosing regimens in an extension of Study 15-HG-0068
Stage 4	All available data, including the additional TID dosing pharmacokinetic data generated during extension conducted in same patients from Study 15-HG-0068	Finalize pharmacokinetic model

*BID* twice daily, *TID* three times daily

precision as measured by the relative standard error (%RSE); graphical examination of standard diagnostic and population analysis goodness-of-fit plots (observed versus both population and individual post-hoc predicted data; conditional weighted residuals [CWRES] versus time since last dose and population predictions; and individual weighted residuals [IWRES] versus individual post-hoc predictions); graphical examination of the agreement between the observed and individual post-hoc predicted data over time or time since last dose (individual observed and predicted overlays); reduction in both residual variability (RV or  $\sigma^2$ ) and interindividual variability (IIV or  $\omega^2$ ); and comparison of the minimum value of the NONMEM objective function (MVOF) for nested models or Akaike's Information Criterion (AIC) for non-nested models [21].

### 2.3.3 Structural Population Pharmacokinetic Model Development Using Single-Dose Data from Study 12-HG-0207

The intensive-sampling pharmacokinetic data from subjects with GNE myopathy from Study 12-HG-0207 was first used to construct a structural population pharmacokinetic model to simultaneously describe the time-course of ManNAc and Neu5Ac concentrations in plasma following single-dose oral administration of ManNAc. A one-compartment model parameterized using a first-order absorption rate-constant of exogenous ManNAc ( $k_a$ , in  $\text{h}^{-1}$ ), an initial endogenous plasma ManNAc concentration ( $M_0$ , in  $\text{ng/mL}$ ), the apparent volume of distribution for ManNAc ( $V_M/F$ , in L), and the apparent clearance of ManNAc ( $CL_M/F$ , in L/h) was fit to the data. The zero-order endogenous production rate constant for ManNAc ( $k_{\text{syn}}$ , in  $\mu\text{g/h}$ ) was calculated as the product of  $M_0$  and  $CL_M/F$ . During structural model development, different types of absorption models to account for slow or delayed oral absorption of ManNAc were explored (e.g., inclusion of absorption lag-time and evaluation of absorption transit compartments). The oral bioavailability ( $F$ ) for ManNAc was not identifiable without pharmacokinetic data following intravenously administered ManNAc and was thus fixed to a value of 1. During the analysis, the relative oral bioavailability ( $F$ ), where  $F$  for a reference dose of 6 g was set equal to 1, was assessed as a power function of ManNAc dose to account for deviation in dose-proportional pharmacokinetics.

An indirect response model approach [22] was utilized to characterize Neu5Ac pharmacokinetics, either with or without a precursor compartment to introduce a delay in Neu5Ac formation, and the model was used to account for increases in Neu5Ac measured in the plasma. This extracellular space concentration theoretically reflects an increase in the intracellular Neu5Ac since that is where the conversion occurs and subsequently Neu5Ac can be transported out of cells through a yet unknown mechanism. The initial Neu5Ac concentration

( $N_0$ , in  $\text{ng/mL}$ ) and the first-order elimination rate constant for Neu5Ac ( $k_{\text{out}}$ , in  $\text{h}^{-1}$ ) were estimated. The zero-order Neu5Ac production rate constant ( $k_{\text{pro}}$ , in  $\text{ng/mL}\cdot\text{h}$ ) for the precursor Neu5Ac compartment (referred to as the Pre-Neu5Ac CMT in model diagram) was calculated. Since there are no direct measurements obtained from the Pre-Neu5Ac CMT, it would not be structurally identifiable to estimate a separate conversion transfer rate constant for pre-Neu5Ac to the Neu5Ac compartments and elimination rate constant for Neu5Ac. Thus, like traditional transit compartment models, both these parameters are assigned the same value ( $k_{\text{out}}$ ) to avoid identifiability issues. The stimulation of  $k_{\text{pro}}$  was evaluated as both a Hill-type function and a reduced linear function. In the Hill-type function, the maximum increase in  $k_{\text{pro}}$  ( $S_{\text{max}}$ ) and plasma ManNAc concentration resulting in 50% of  $S_{\text{max}}$  ( $SC_{50}$ , in  $\text{ng/mL}$ ) were estimated. In the reduced linear model, an effect slope (SLP) was instead estimated.

Interindividual variability was estimated for selected structural pharmacokinetic model parameters using exponential error models, assuming these parameters were log-normally distributed. For residual variability, separate combined additive plus constant coefficient of variation (CCV) error models were estimated for both ManNAc and Neu5Ac. The additive plus CCV residual variability model was reduced to only a CCV error model by fixing the additive term to zero if it was shown that the absolute value of the individual weighted residuals (absolute IWRES) was constant when examined graphically over the range of individual predicted concentrations or if the additive component was estimated to be negligible.

### 2.3.4 Update of Structural Population Pharmacokinetic Model Development Using Both Single-Dose and Repeated Dosing Data Followed by Covariate Analysis

The structural population pharmacokinetic model (Stage 1) was updated by including the pharmacokinetic sampling data from 1 year of repeated twice daily dosing of ManNAc in subjects with GNE myopathy from Study 15-HG-0068. Several feedback mechanisms were evaluated to describe apparent time-varying changes in ManNAc and Neu5Ac pharmacokinetics upon repeated dosing, including (i) Neu5Ac concentration-dependent increases in enzymatic conversion of ManNAc to Neu5Ac; (ii) Neu5Ac concentration-dependent decrease in endogenous production of ManNAc; or (iii) time-dependent increases in enzymatic conversion of ManNAc to Neu5Ac. During model development, the latter mechanism was determined to provide the best fit to the data and this involved allowing the SLP parameter to increase exponentially over time from an initial value ( $SLP_0$ ) to a new steady-state value ( $SLP_{SS}$ ).

A formal covariate analysis was then performed using stepwise forward selection ( $\alpha = 0.01$ ) and stepwise backward

elimination ( $\alpha = 0.001$ ); additional details are provided in Online Resource 3 (see ESM).

The updated base structural population pharmacokinetic model, including any statistically significant covariate effects, was evaluated as previously described in the Pharmacokinetic Model Building section of this manuscript. In addition, the overall distribution of the normalized prediction distribution errors (NPDE) provided by NONMEM was compared with a normal distribution to determine if the residual variability models were biased. The distribution of  $\eta$  for each parameter was also examined for irregularities (e.g., skewness and bi-modalities) and alternative IIV models or transformations (e.g., Box-Cox) were considered if necessary.

The updated population pharmacokinetic model was also evaluated by performing dose- and day-stratified visual predictive checks (VPCs). This procedure graphically examined the agreement between the 10th, 50th, and 90th percentiles of the observed and simulated pharmacokinetic concentrations across time intervals [23]. Based upon graphical review of these plots, the population pharmacokinetic model was refined as appropriate to try to correct any substantial issues with respect to the fixed or random effects parameters in the model if there was discordance between the 10th, 50th, and 90th percentiles of the observed and the simulated pharmacokinetic data.

### 2.3.5 Simulations to Evaluate Potential ManNAc Dosing Regimens for Subjects with GNE Myopathy

Simulations were performed within an R Shiny application using the updated population pharmacokinetic model to generate ManNAc and Neu5Ac concentration–time profiles for various ManNAc dosing regimens in order to guide dose selection for future clinical trials of ManNAc in subjects with GNE myopathy. A single clinical trial was simulated in which 90 virtual subjects were generated, having the same demographic, clinical laboratory, and disease-related characteristics as the subjects with GNE myopathy used to develop the population pharmacokinetic model for ManNAc and Neu5Ac. Several oral ManNAc dosing regimens (3, 4, 6, and 10 g) administered either every 8 h (Q8H), every 12 h (Q12H), or every 24 h (Q24H) were simulated for 30 days in subjects with GNE myopathy (further details provided in Online Resource 4, see ESM). Based on these simulations, serial blood samples for plasma ManNAc and Neu5Ac concentration-versus-time curves were obtained in eight subjects with GNE myopathy who received a ManNAc dosing regimen of 4 g TID as part of the extension phase of Study 15-HG-0068.

### 2.3.6 Final Population Pharmacokinetic Model

The final population pharmacokinetic model was lastly derived after including the additional pharmacokinetic sampling data obtained at an extension visit during day 912 in which, after a 7-day washout period, subjects with GNE myopathy from Study 15-HG-0068 received ManNAc at doses of 4 g TID. The population pharmacokinetic parameters were re-estimated and all of the same model discrimination and evaluation criteria (precision of model parameter estimates as well as examination of goodness-of-fit plots, individual predicted overlays, VPCs, etc.) were reviewed.

## 3 Results

### 3.1 Subject Demographics

Of the 34 subjects with GNE myopathy included in the model, 16 were male and 18 were female. The majority (70.6%) were Caucasian and 26.5% were Asian. The mean (SD) age was 41.3 (10.4) years, weight was 83.5 (20.2) kg, body mass index was 27.6 (4.7) kg/m<sup>2</sup>, and mean albumin value was 3.8 (0.4) g/dL. Subjects had normal renal function with mean eGFR of 123 mL/min (CKD-EPI cystatin C equation) [18]. Descriptive demographics and baseline characteristics are presented in Table 2. All subjects had genetic confirmation of GNE myopathy by identification of biallelic pathogenic variants in the *GNE* gene. The majority of subjects were compound heterozygotes for an epimerase and a kinase domain mutation (67.6%) or two kinase domain mutations (23.5%).

### 3.2 Pharmacokinetic Data Assembly and Description

After completion of all dataset assembly activities, a total of 773 ManNAc and 777 Neu5Ac concentrations in plasma collected from 34 subjects with GNE myopathy across both studies were available for developing the original population pharmacokinetic model. A total of four plasma ManNAc concentrations were identified as potential outliers and were excluded from the population pharmacokinetic analysis. An additional 72 ManNAc and 72 Neu5Ac concentrations were later added during the final population pharmacokinetic modeling stage following repeated dosing of ManNAc in Study 15-HG-0068 beyond 1 year, including data from 4-g TID dosing obtained during the extension phase.

**Table 2** Demographics and baseline characteristics for the pharmacokinetic analysis subject population ( $n = 34$ )

Variable	<i>N</i> (%)	Mean	SD	Median	Min	Max
Age (years)	34	41.3	10.4	39.5	25	65
Weight (kg)	34	83.5	20.2	84.6	49.3	115
Height (cm)	34	173	13.3	172	151	197
BMI (kg/m <sup>2</sup> )	34	27.6	4.7	27.2	19.1	39.8
BSA (m <sup>2</sup> )	34	2.01	0.31	2.06	1.45	2.50
eGFR (mL/min) <sup>a</sup>	34	123	22.2	120	85.0	170
Albumin (g/dL)	34	3.83	0.403	3.80	3.2	4.8
Serum creatinine (mg/dL)	34	0.499	0.223	0.49	0.12	0.95
Creatine kinase (U/L)	34	236	124	220	44.0	556
Sex						
Male	16 (47.1)					
Female	18 (52.9)					
Race						
Caucasian	24 (70.6)					
Asian	8 (26.5)					
Other	2 (2.94)					
GNE domain mutations						
Epimerase/kinase	23 (67.6)					
Kinase/kinase	8 (23.5)					
Deletion/kinase	2 (5.88)					
Epimerase/epimerase	1 (2.94)					

<sup>a</sup>eGFR using the CKD-EPI cystatin C equation[19]

### 3.3 Pharmacokinetic Model

#### 3.3.1 Structural Pharmacokinetic Model Development Using Single-Dose Data from Subjects with GNE Myopathy in Study 12-HG-0207

Several variations of the aforementioned structural pharmacokinetic model were evaluated to jointly characterize the plasma ManNAc and Neu5Ac concentrations in subjects with GNE myopathy who received a single dose of ManNAc in Study 12-HG-0207. The best structural pharmacokinetic model featured (i) an absorption lag-time for ManNAc; (ii) a precursor compartment for Neu5Ac formation; and (iii) allowed relative oral bioavailability to nonlinearly decrease with ManNAc dose using a power function, which was hypothesized to result from either dose-limiting solubility or incomplete absorption of ManNAc at higher doses.

#### 3.3.2 Update of Structural Pharmacokinetic Model Using Repeated-Dosing Data from Subjects with GNE Myopathy in Study 15-HG-0068

The base structural pharmacokinetic model developed in subjects with GNE myopathy who received a single-dose of ManNAc in Study 12-HG-0207 was updated after including additional data from subjects with GNE myopathy who received repeated doses of ManNAc in Study 15-HG-0068.

During this stage, inter-occasion variability (IOV) was evaluated for several parameters (including  $k_a$ ,  $CL_M/F$ ,  $V_M/F$ , and SLP) since intensive pharmacokinetic sampling data were available on multiple days of treatment. The pharmacokinetic occasions were defined as follows based upon periods when intensive-sampling pharmacokinetic data were available: Occasion 1 encompassed any data prior to Day 4 relative to the start of treatment; Occasion 2 encompassed any data between Day 4 and Day 30 relative to the start of treatment; and Occasion 3 encompassed any data after Day 30 relative to the start of treatment. The SLP parameter, representing the efficiency of enzymatic conversion of ManNAc to Neu5Ac, appeared to increase upon repeated dosing on days with intensive pharmacokinetic sampling (Occasions 2 and 3 relative to Occasion 1). This suggested a systematic increase in the conversion of ManNAc to Neu5Ac across subjects and dose groups upon repeated dosing, which was best handled in the model using a time-dependent increase in SLP from an initial value ( $SLP_0$ ) to a new steady-state value ( $SLP_{SS}$ ) using a first-order rate constant ( $k_{inc}$ , in  $h^{-1}$ ). After this change in model structure was implemented, IOV was only retained on  $CL_M/F$  to avoid overparameterization.

#### 3.3.3 Covariate Analysis

A graphical screening procedure was conducted to examine the relationship between subject covariate effects and

key model parameters prior to Step 1 of forward selection. Plots were generated of the individual post-hoc parameter minus the population mean parameter versus patient covariates using the base structural population pharmacokinetic model. Based upon this graphical screening procedure, only selected patient covariate–parameter relationships were formally tested within NONMEM, none of which appeared to be very strong parameter–covariate relationships. In Step 1 of forward selection, as summarized in Online Resource 5 (see ESM), none of the parameter–covariate relationships tested were statistically significant ( $p > 0.01$ ). Therefore, forward selection was concluded, and no covariates were added to the base structural model.

### 3.3.4 Simulations Using Updated Structural Pharmacokinetic Model

Simulations were performed using the updated structural population pharmacokinetic model to generate pharmacokinetic data for a prospective new study in subjects with GNE myopathy ( $N = 90$ ). Summary statistics for average drug concentration at steady state ( $C_{ss,ave}$ , in ng/mL) for various ManNAc Q8H, Q12H, or Q24H dosing regimens administered for 30 days in subjects with GNE myopathy are provided in Table 3. These simulations demonstrated that for a planned 12-g-per-day dose, administration of 4 g Q8H would be expected to provide a greater Neu5Ac  $C_{ss,ave}$  than administering 6 g Q12H (702 vs 612 ng/mL) based upon the greater relative oral bioavailability predicted from the population pharmacokinetic model. Based upon these findings, an extension visit (Day 912) was added to Study 15-HG-0068 in which subjects who volunteered to continue ManNAc treatment received ManNAc at doses of 4 g Q8H after a 7-day interruption of ManNAc treatment to evaluate pharmacokinetic parameters of this dosing regimen.

### 3.3.5 Final Population Pharmacokinetic Model

The final population pharmacokinetic model (Fig. 2; Table 4, Supplemental Model Code in Online Resource 6, see ESM) was then generated after including newly generated pharmacokinetic data from Study 15-HG-0068, in which a total of eight subjects who completed a 7-day interruption of ManNAc treatment went on to further receive ManNAc 4 g Q8H starting on approximately Day 912. The final model describing the amount of ManNAc dosed ( $A_{PO}$ ), plasma ManNAc amounts ( $A_M$ ) and concentrations ( $M = A_M/V_M$ ), plasma pre-cursor Neu5Ac concentrations (PN), and plasma Neu5Ac concentrations utilized the following differential equations along with their respective initial conditions (IC):

$$\frac{dA_{PO}}{dt} = -k_a \cdot A_{PO}, \text{ IC} = \text{Dose} \quad (1)$$

$$\frac{dA_M}{dt} = k_{syn} + k_a \cdot A_{PO} - \frac{CL_M}{V_M} \cdot A_M, \text{ IC} = V_M \cdot M_0 \quad (2)$$

$$\frac{dPN}{dt} = k_{pro} \cdot (1 + SLP \cdot M) - k_{out} \cdot PN, \text{ IC} = N_0 \quad (3)$$

$$\frac{dN}{dt} = k_{out} \cdot PN - k_{out} \cdot N, \text{ IC} = N_0 \quad (4)$$

The baseline condition was assumed to be stationary, and so the zero-order production of PN was defined as

$$k_{pro} = \frac{k_{out} \cdot N_0}{(1 + SLP_0 \cdot M_0)} \quad (5)$$

The linear stimulation constant for the conversion of ManNAc (SLP) was defined as

**Table 3** Summary statistics for  $C_{ss,ave}$  in ng/mL for various ManNAc dosing regimens in subjects with GNE myopathy ( $N = 90$ )

ManNAc dose	Q8H for 30 days		Q12H for 30 days		Q24H for 30 days	
	Median	5th–95th percentiles	Median	5th–95th percentiles	Median	5th–95th percentiles
Plasma ManNAc $C_{ss,ave}$ (ng/mL)						
3 g	922	501–1550	642	359–1060	365	223–570
4 g	1060	573–1790	729	404–1220	411	246–650
6 g	1290	692–2180	881	480–1480	483	281–780
10 g	1650	883–2810	1120	607–1900	603	340–989
Plasma Neu5Ac $C_{ss,ave}$ (ng/mL)						
3 g	633	247–2010	484	209–1420	338	174–825
4 g	702	265–2300	533	222–1610	364	181–921
6 g	818	296–2780	612	242–1930	405	190–1080
10 g	1020	344–3540	735	274–2440	464	204–1330

Dosing regimens: Q8H every 8 h, Q12H every 12 hours, Q24H once daily

$C_{ss,ave}$  average drug concentration at steady state

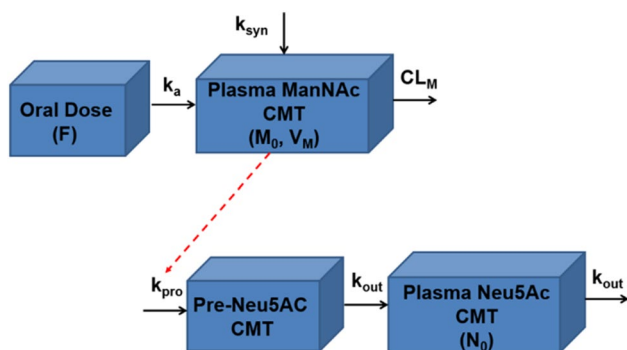


**Fig. 2** Diagram of final structural pharmacokinetic model for ManNAc and Neu5Ac.  $F$  oral bioavailability,  $k_a$  first-order oral absorption rate-constant for exogenously administered ManNAc ( $\text{h}^{-1}$ ),  $k_{\text{syn}}$  zero-order endogenous production rate constant for ManNAc ( $\mu\text{g}/\text{h}$ ),  $\text{CMT}$  compartment,  $\text{CL}_M$  apparent clearance for ManNAc ( $\text{L}/\text{h}$ ),  $M_0$  initial endogenous plasma ManNAc concentration ( $\text{ng}/\text{mL}$ ),  $V_M$  apparent volume of distribution for ManNAc ( $\text{L}$ ),  $k_{\text{pro}}$  zero-order production rate constant for Neu5Ac in precursor compartment ( $\text{ng}/\text{mL}\cdot\text{h}$ ),  $\text{Pre-Neu5Ac}$  Neu5Ac precursor,  $k_{\text{out}}$  first-order elimination rate constant for Neu5Ac ( $\text{h}^{-1}$ ),  $N_0$  initial endogenous plasma Neu5Ac concentration ( $\text{ng}/\text{mL}$ )

$$\text{SLP} = \text{SLP}_{\text{SS}} - (\text{SLP}_{\text{SS}} - \text{SLP}_0) \cdot \exp^{-k_{\text{inc}} \cdot t} \quad (6)$$

Several changes were made to the structural population pharmacokinetic model at this stage of the analysis. The Q8H dosing period was assigned a separate occasion when estimating IOV on  $\text{CL}_M/F$ , which slightly improved model fit. In addition, the IIV on  $k_{\text{out}}$  was estimated to be negligible and was no longer retained as part of the final population pharmacokinetic model. Lastly, it was now possible to achieve model convergence when estimating the effect of ManNAc dose on  $F$  (previously this parameter was fixed to the final estimate of a preliminary run in order to achieve successful minimization).

The population mean pharmacokinetic parameter estimates for the fit of the final updated population pharmacokinetic model to the data from subjects with GNE myopathy who received a single dose of ManNAc in Study 12-HG-0207 or repeated doses of ManNAc in Study 15-HG-0068 are provided in Table 4. The  $M_0$  and  $N_0$  parameters were consistent with previously reported values of plasma ManNAc and Neu5Ac in subjects with GNE myopathy [11]. Given the relatively small number of subjects, the precision for the IIV terms improved but still were not estimated very precisely. Goodness-of-fit plots demonstrated an acceptable and unbiased fit to the data as shown for plasma ManNAc concentrations in Online Resource 7 and for plasma Neu5Ac concentrations in Online Resource 8 (see ESM). There was reasonably acceptable agreement between the observed plasma

**Table 4** Final population pharmacokinetic model parameter estimates for ManNAc and Neu5Ac in subjects with GNE myopathy

Parameter	Final typical value estimate	%SEM
$k_a$ ( $\text{h}^{-1}$ )	0.256	15.2
$\text{CL}_M/F$ ( $\text{L}/\text{h}$ )	631	14.8
$V_M/F$ ( $\text{L}$ )	506	29.4
$M_0$ ( $\text{ng}/\text{mL}$ )	61.1	12.0
$N_0$ ( $\text{ng}/\text{mL}$ )	150	5.71
$k_{\text{out}}$ ( $\text{h}^{-1}$ )	0.283	5.65
$\text{SLP}_0$ ( $\text{ng}/\text{mL}$ ) $^{-1}$	0.000619	29.1
$\text{SLP}_{\text{SS}}$ ( $\text{ng}/\text{mL}$ ) $^{-1}$	0.00334	35.0
$k_{\text{inc}}$ ( $\text{h}^{-1}$ )	0.0287	45.3
$t_{\text{lag}}$ ( $\text{h}$ )	0.254	26.4
$k_{\text{syn}}$ ( $\mu\text{g}/\text{h}$ ) <sup>a</sup>	38,554	N/A
$k_{\text{pro}}$ ( $\text{ng}/\text{mL}\cdot\text{h}$ ) <sup>a</sup>	40.9	N/A
Relative ManNAc bio-availability ( $F$ )		
$F$ for 6 g dose	1	Fixed
$F$ -Dose slope	-0.405	39.0
$\omega^2$ for $k_a$	0.0697 (26.4% CV)	91.4
$\omega^2$ for $\text{CL}_M/F$	0.0636 (25.2% CV)	93.2
$\omega^2$ for $V_M/F$	0.120 (34.6% CV)	170
$\omega^2$ for $M_0$	0.0966 (31.1% CV)	43.5
$\omega^2$ for $N_0$	0.0439 (21.0% CV)	55.4
$\omega^2$ for $\text{SLP}_{\text{SS}}$	0.383 (61.9% CV)	130
IOV on $\text{CL}_M/F$	0.0580 (24.1% CV)	63.6
$\sigma^2$ CCV component	0.102 (31.9% CV)	8.13
Additive component	0.0370 (19.2% CV)	5.68

$\text{CL}_M$  apparent clearance for ManNAc,  $F$  oral bioavailability,  $k_a$  first-order oral absorption rate-constant for exogenously administered ManNAc,  $k_{\text{inc}}$  first-order rate-constant of increase in the rate of conversion from ManNAc to Neu5Ac,  $k_{\text{out}}$  first-order elimination rate constant for Neu5Ac ( $\text{h}^{-1}$ ),  $k_{\text{pro}}$  zero-order production rate constant for Neu5Ac in precursor compartment,  $k_{\text{syn}}$  zero-order endogenous production rate constant for ManNAc,  $M_0$  initial endogenous plasma ManNAc concentration,  $N_0$  initial endogenous plasma Neu5Ac concentration,  $t_{\text{lag}}$  absorption lag-time of ManNAc,  $V_M/F$  apparent volume of distribution for ManNAc

<sup>a</sup> $k_{\text{syn}}$  and  $k_{\text{pro}}$  are secondary parameters, where a typical value was calculated from typical values for other primary parameters

ManNAc concentrations and both the population and individual predicted concentrations ( $r^2 = 0.75$  and  $r^2 = 0.89$ , respectively). There was also reasonably acceptable agreement between the observed plasma Neu5Ac concentrations and both the population and individual predicted concentrations ( $r^2 = 0.68$  and  $r^2 = 0.86$ , respectively). An updated plot of the relative oral bioavailability versus ManNAc dose (Online Resource 9, see ESM) demonstrated that the relative oral bioavailability ( $F$ ) ranged from 1.32 at a dose of 3 g to 0.81 at a dose of 10 g (with



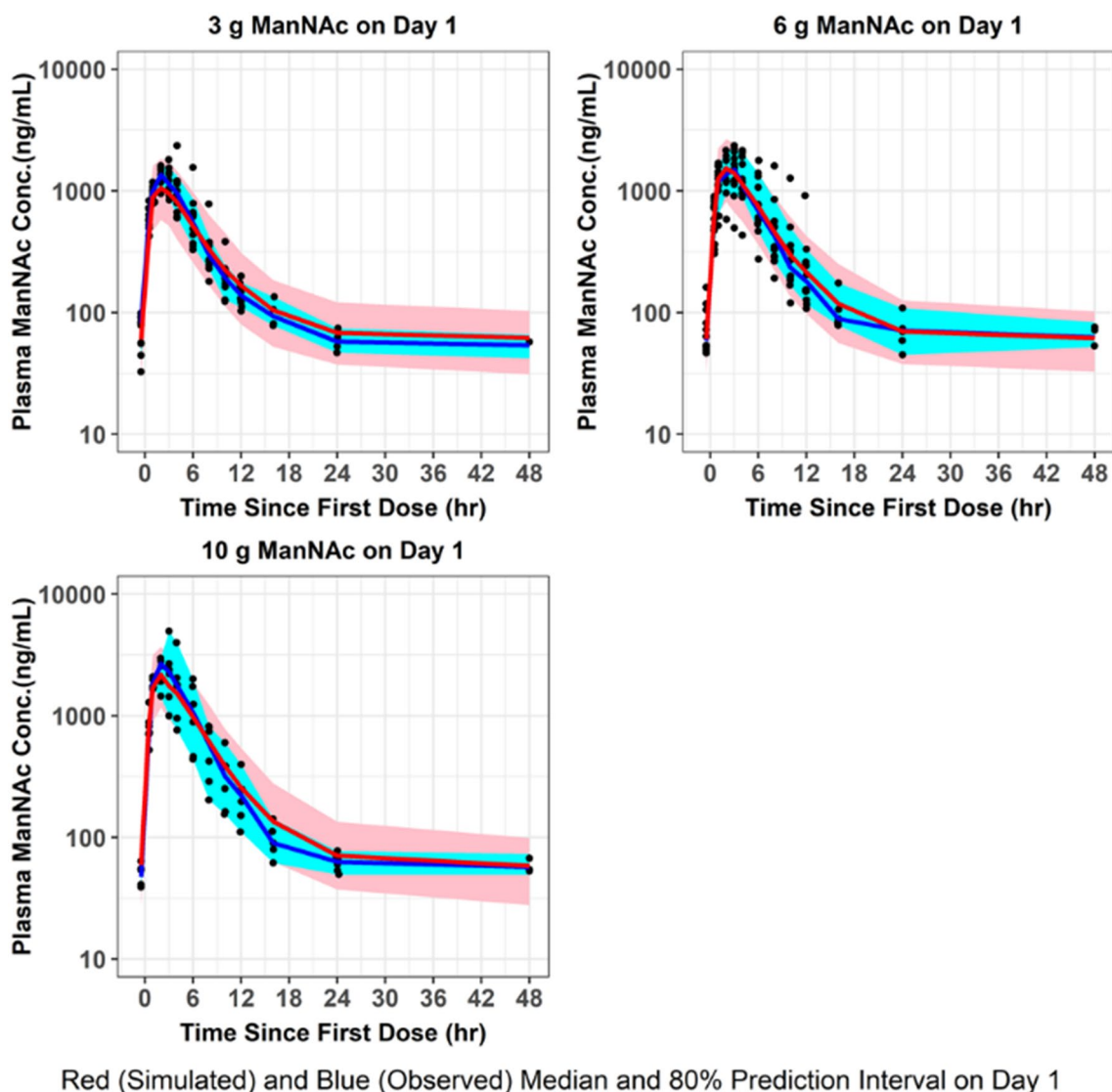


**Fig. 3** VPC for plasma ManNAc concentrations. The final population pharmacokinetic model was used to generate VPCs, stratified by ManNAc dose group, following single-dose administration of ManNAc to subjects with GNE myopathy. VPCs visual predictive checks

6-g dose serving as reference value where  $F = 1$ ). Lastly, an updated plot of the conversion slope of ManNAc to Neu5Ac (increase in SLP from  $SLP_0$  to  $SLP_{ss}$ ) for the final population pharmacokinetic model fit is shown in Online Resource 10 (see ESM). This demonstrated that after about 1 week, the SLP parameter reaches steady-state levels. VPCs were performed for plasma ManNAc and Neu5Ac concentrations using the final population pharmacokinetic model following administration of a single dose (Figs. 3, 4) or repeated doses (Figs. 5, 6) of ManNAc to subjects with GNE myopathy and demonstrated reasonable agreement between the 5th, 50th and 95th percentiles of the observed and simulated data.

## 4 Discussion

GNE myopathy is a genetic muscle disease with no approved therapy. Currently, ManNAc is the only drug in clinical development for this orphan disease [2]. Similar to other orphan drug development programs, the limited number of subjects and data available complicate evidence-based decisions during the clinical development stage, such as the selection of drug dose levels and frequency of administration, which is critical for safety and ensuring therapeutic doses are tested in clinical trials. The use of tools such as population pharmacokinetic modeling can facilitate decision making during drug development for rare diseases.

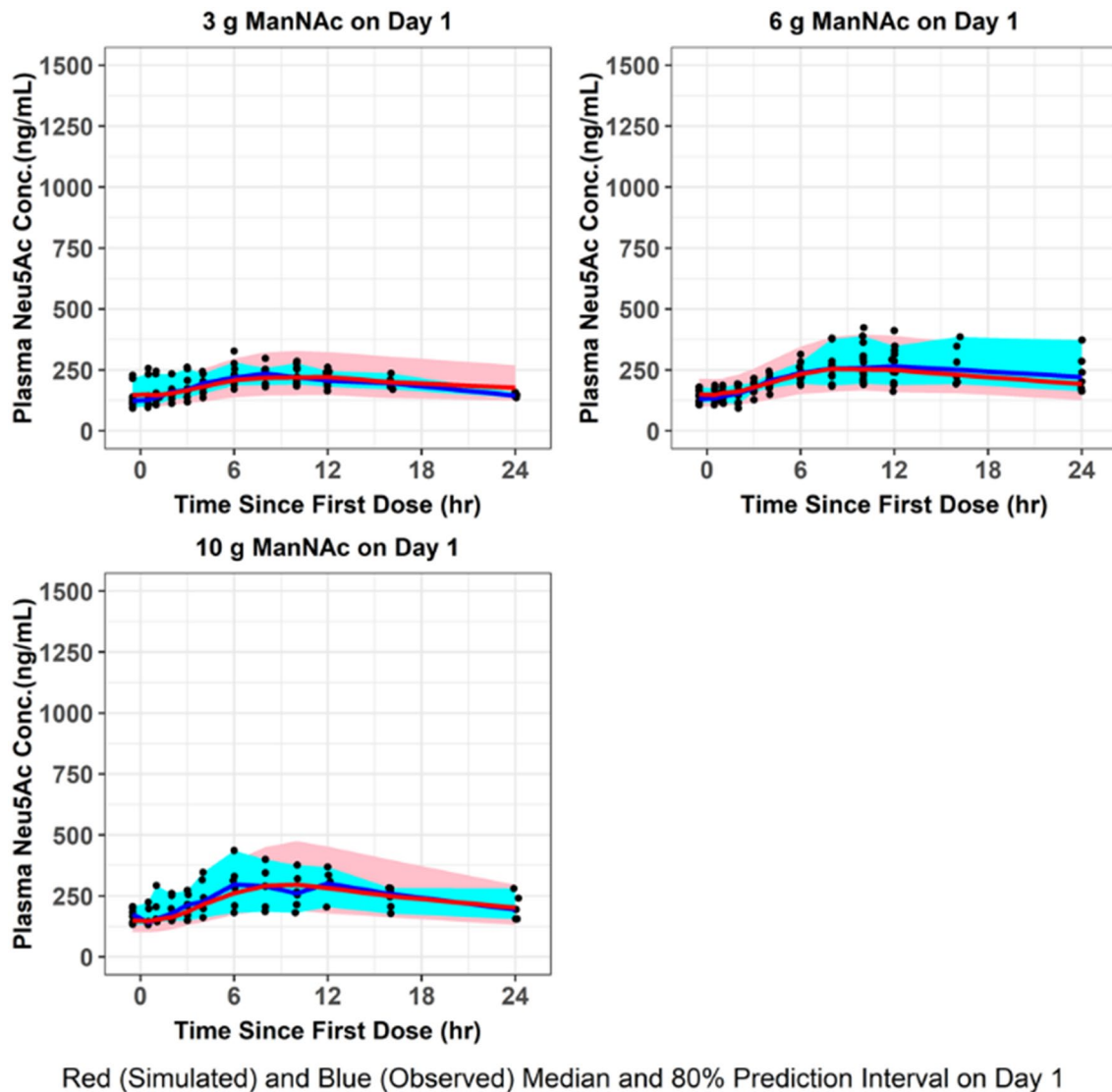


**Fig. 4** VPC for plasma Neu5Ac concentrations. The final population pharmacokinetic model was used to generate VPCs, stratified by ManNAc dose group, following single-dose administration of ManNAc to subjects with GNE myopathy. VPCs visual predictive checks

Methods have been described in the literature to increase the sialylation of glycoproteins in mammalian cell cultures [4, 8, 14]. One method, which bypasses the rate-limiting step in the production of sialic acids, is exogenous supplementation of ManNAc (Fig. 1). Biosynthesis along the sialic acid pathway can continue in those with severe ManNAc kinase deficiency by utilizing the ancillary enzyme GlcNAc kinase [11, 24]. When evaluating pups from homozygous mutant (*Gne*<sup>M712T/M712T</sup>) mice, exogenously administered ManNAc (supplemented water to breeding pairs and nursing females) increased GNE enzyme activity in the muscle in pups at postnatal Day 2 from ~19 to 31% of untreated wild-type mean values ( $p = 0.05$ ) [17].

Here, we describe the development of a robust population pharmacokinetic model to simultaneously characterize plasma ManNAc and Neu5Ac concentrations following oral administration of ManNAc to subjects with GNE myopathy. This semi-mechanistic model was developed as part of an iterative process that refined the model as data were accumulated. For example, a time-dependent increase in the efficiency of conversion of ManNAc to Neu5Ac was incorporated to better fit the data upon repeated dosing, which was subsequently collapsed from a capacity limited Hill-type function to a linear slope term due to parameter identifiability issues.

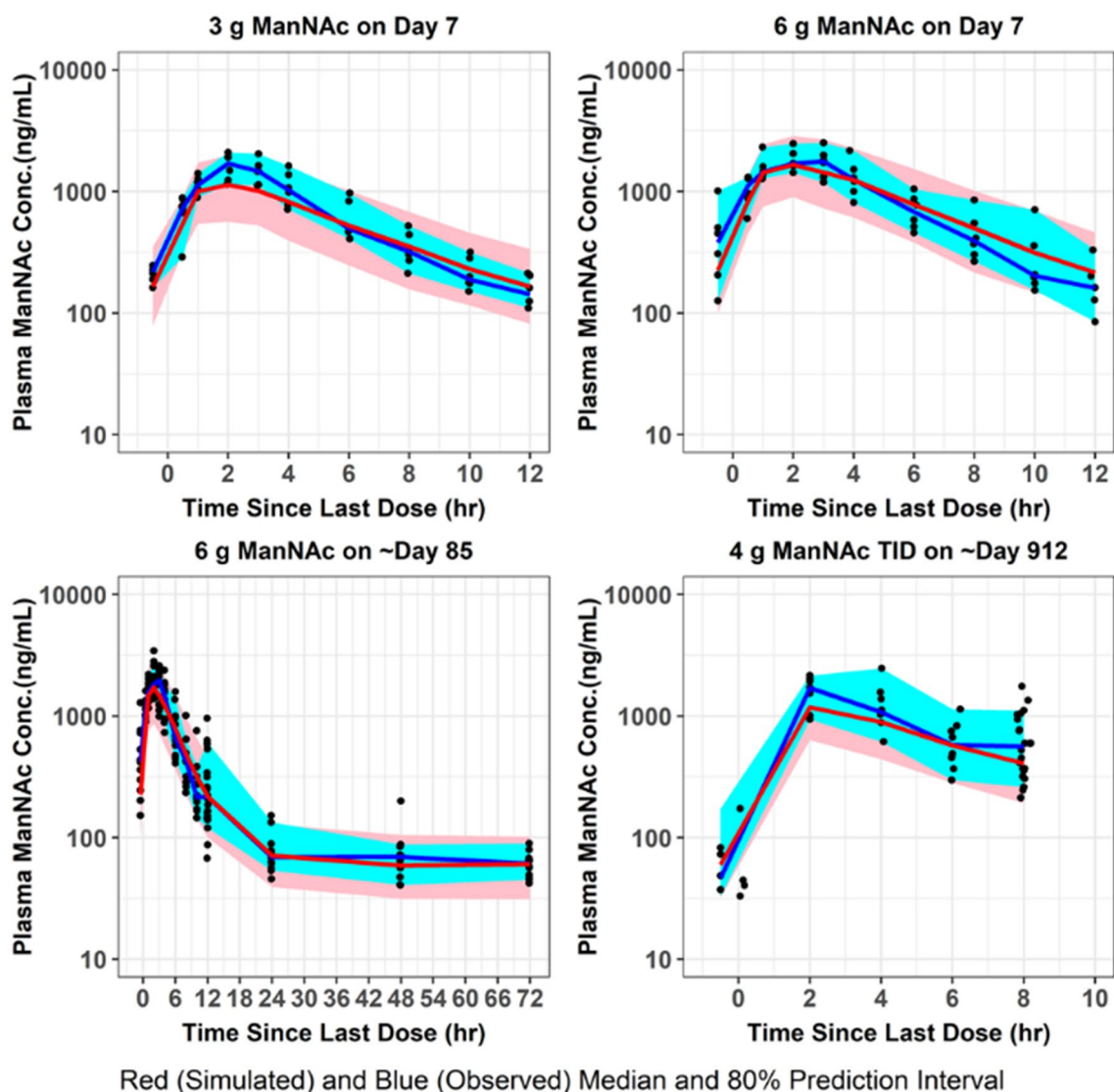


**Fig. 5** VPC for plasma ManNAc concentrations. The final population pharmacokinetic model was used to generate VPCs, stratified by ManNAc dose group, following repeated-dose administration of ManNAc to subjects with GNE myopathy. VPCs visual predictive checks

The parameter estimates for M0 and N0 were consistent with previously reported baseline values for plasma ManNAc and Neu5Ac in subjects with GNE myopathy [11]. The endogenous levels of plasma ManNAc and Neu5Ac measured in normal plasma during the development of the bioanalytical method were approximately 50 ng/mL and 159 ng/mL, respectively [20], although reference intervals have not been established. As seen in Table 2, the plasma levels of Neu5Ac achieved after ManNAc administration suggest the restoration of the Neu5Ac intracellular pathway in these subjects with GNE myopathy, as previously shown [11].

The population pharmacokinetic model was useful in identifying dosing regimens to increase ManNAc

bioavailability with the potential to improve gastrointestinal tolerability. The pharmacokinetic and safety data in subjects with GNE myopathy had suggested that there may be incomplete absorption at higher ManNAc doses, as evidenced by the fact that there was an increased incidence of gastrointestinal adverse events as ManNAc dose increased. To mimic incomplete absorption, the relative oral bioavailability of ManNAc was modeled as a non-linear function of ManNAc dose. Preliminary simulations suggested that the relative oral bioavailability of ManNAc could be increased with more frequent dosing of lower dose levels, such as giving the same daily dose of 12 g divided into 4 g Q8H rather than 6 g Q12H (Table 3). This was confirmed by pharmacokinetic evaluations of a

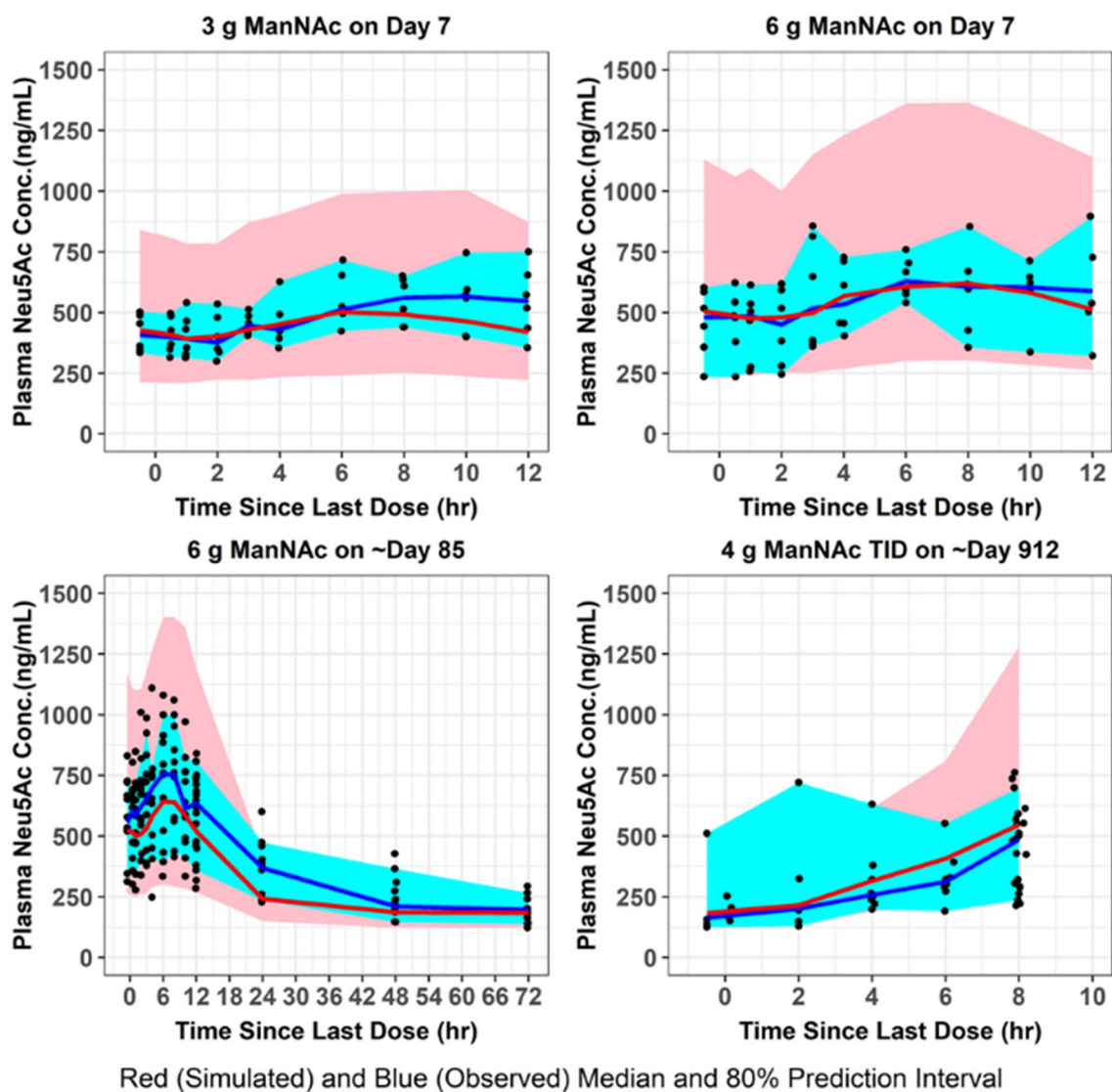


**Fig. 6** VPC for plasma Neu5Ac concentrations. The final population pharmacokinetic model was used to generate VPCs, stratified by ManNAc dose group, following repeated-dose administration of ManNAc to subjects with GNE myopathy. VPCs visual predictive checks

4-g Q8H regimen later studied in subjects with GNE myopathy, which showed that measured plasma ManNAc and Neu5Ac concentrations were generally consistent with the model predictions.

## 5 Conclusions

A semi-mechanistic population pharmacokinetic model was developed to simultaneously characterize plasma ManNAc and its metabolite Neu5Ac following oral administration of ManNAc to subjects with GNE myopathy. This population pharmacokinetic model is a useful tool in the clinical drug development of ManNAc to guide

dose selection and understand the effects of oral ManNAc administration on Neu5Ac production and exposure.

**Supplementary Information** The online version contains supplementary material available at <https://doi.org/10.1007/s40268-021-00343-6>.

## Declarations

**Funding** This study was supported by the Intramural Research Program of the National Human Genome Research Institute (NHGRI), National Institutes of Health, Bethesda, Maryland, United States and by a Cooperative Research and Development Agreement with Escala Therapeutics, Inc.

**Conflict of interest** This study was partially funded through Cooperative Research and Development Agreements (CRADA) with Escala

Therapeutics, Inc. Dr Huizing is a co-inventor on patent US Patent No. 8,410,063. “*N*-acetylmannosamine as a Therapeutic Agent”.

**Ethics approval** The protocols were approved by the National Human Genome Research Institute (NHGRI) Institutional Review Board (IRB).

**Consent to participate** All subjects provided written, informed consent.

**Consent for publication** Not applicable.

**Availability of data and materials** Data is available upon request.

**Code availability** NONMEM model code provided in Supplemental File.

**Author contributions** Nuria Carrillo and Marjan Huizing were involved in study planning, conduct and data collection as well as manuscript preparation. Scott Van Wart, Donald E. Mager, and Cindy Bednasz were involved with study planning, data analysis and manuscript writing. All authors read and approved the final manuscript.

**Open Access** This article is licensed under a Creative Commons Attribution-NonCommercial 4.0 International License, which permits any non-commercial use, sharing, adaptation, distribution and reproduction in any medium or format, as long as you give appropriate credit to the original author(s) and the source, provide a link to the Creative Commons licence, and indicate if changes were made. The images or other third party material in this article are included in the article’s Creative Commons licence, unless indicated otherwise in a credit line to the material. If material is not included in the article’s Creative Commons licence and your intended use is not permitted by statutory regulation or exceeds the permitted use, you will need to obtain permission directly from the copyright holder. To view a copy of this licence, visit <http://creativecommons.org/licenses/by-nc/4.0/>.

## References

- Huizing M, Malicdan MV, Krasnewich DM, Manoli I, Carrillo-Carrasco N. GNE myopathy. In: Valle D, Antonarakis S, Ballabio A, Beaudet A, Mitchell GA, editors. The online metabolic and molecular bases of inherited disease. New York: McGraw-Hill; <http://ommbidmhmedical.com/content.aspx?bookid=2709&sectionid=225900450>. Accessed 18 Mar 2020.
- Carrillo N, Malicdan MC, Huizing M. GNE myopathy: etiology, diagnosis, and therapeutic challenges. *Neurotherapeutics*. 2018;15(4):900–14. <https://doi.org/10.1007/s13311-018-0671-y>.
- Eisenberg I, Avidan N, Potikha T, Hochner H, Chen M, Olender T, et al. The UDP-*N*-acetylglucosamine 2-epimerase/*N*-acetylmannosamine kinase gene is mutated in recessive hereditary inclusion body myopathy. *Nat Genet*. 2001;29(1):83–7. <https://doi.org/10.1038/ng718>.
- Keppeler OT, Hinderlich S, Langner J, Schwartz-Albiez R, Reutter W, Pawlita M. UDP-GlcNAc 2-epimerase: a regulator of cell surface sialylation. *Science*. 1999;284(5418):1372–6. <https://doi.org/10.1126/science.284.5418.1372>.
- Varki A. Diversity in the sialic acids. *Glycobiology*. 1992;2(1):25–40. <https://doi.org/10.1093/glycob/2.1.25>.
- Varki A. Sialic acids in human health and disease. *Trends Mol Med*. 2008;14(8):351–60. <https://doi.org/10.1016/j.molmed.2008.06.002>.
- Gagiannis D, Orthmann A, Danssmann I, Schwarzkopf M, Weidemann W, Horstkorte R. Reduced sialylation status in UDP-*N*-acetylglucosamine-2-epimerase/*N*-acetylmannosamine kinase (GNE)-deficient mice. *Glycoconj J*. 2007;24(2–3):125–30. <https://doi.org/10.1007/s10719-006-9019-7>.
- Noguchi S, Keira Y, Murayama K, Ogawa M, Fujita M, Kawahara G, et al. Reduction of UDP-*N*-acetylglucosamine 2-epimerase/*N*-acetylmannosamine kinase activity and sialylation in distal myopathy with rimmed vacuoles. *J Biol Chem*. 2004;279(12):11402–7. <https://doi.org/10.1074/jbc.M313171200>.
- Tajima Y, Uyama E, Go S, Sato C, Tao N, Kotani M, et al. Distal myopathy with rimmed vacuoles: impaired *O*-glycan formation in muscular glycoproteins. *Am J Pathol*. 2005;166(4):1121–30. [https://doi.org/10.1016/S0002-9440\(10\)62332-2](https://doi.org/10.1016/S0002-9440(10)62332-2).
- Leoyklang P, Class B, Noguchi S, Gahl WA, Carrillo N, Nishino I, et al. Quantification of lectin fluorescence in GNE myopathy muscle biopsies. *Muscle Nerve*. 2018;58(2):286–92. <https://doi.org/10.1002/mus.26135>.
- Xu X, Wang AQ, Latham LL, Celeste F, Ciccone C, Malicdan MC, et al. Safety, pharmacokinetics and sialic acid production after oral administration of *N*-acetylmannosamine (ManNAc) to subjects with GNE myopathy. *Mol Genet Metab*. 2017;122(1–2):126–34. <https://doi.org/10.1016/j.ymgme.2017.04.010>.
- Bardor M, Nguyen DH, Diaz S, Varki A. Mechanism of uptake and incorporation of the non-human sialic acid *N*-glycolylneuraminic acid into human cells. *J Biol Chem*. 2005;280(6):4228–37. <https://doi.org/10.1074/jbc.M412040200>.
- Gilormini PA, Lion C, Vicogne D, Levade T, Potelle S, Mariller C, Guérardel Y, Biot C, Foulquier F. A sequential bioorthogonal dual strategy: ManNAI and SiaNAI as distinct tools to unravel sialic acid metabolic pathways. *Chem Comm*. 2016;52(11):2318–21. <https://doi.org/10.1039/c5cc08838k>.
- Thomas GH, Scocca J, Miller CS, Reynolds LW. Accumulation of *N*-acetylneuraminic acid (sialic acid) in human fibroblasts cultured in the presence of *N*-acetylmannosamine. *Biochim Biophys Acta*. 1985;846(1):37–43. [https://doi.org/10.1016/0167-4889\(85\)90107-7](https://doi.org/10.1016/0167-4889(85)90107-7).
- Seppala R, Lehto VP, Gahl WA. Mutations in the human UDP-*N*-acetylglucosamine 2-epimerase gene define the disease sialuria and the allosteric site of the enzyme. *Am J Hum Genet*. 1999;64(6):1563–9. <https://doi.org/10.1086/302411>.
- Niethamer TK, Yardeni T, Leoyklang P, Ciccone C, Astiz-Martinez A, Jacobs K, et al. Oral monosaccharide therapies to reverse renal and muscle hyposialylation in a mouse model of GNE myopathy. *Mol Genet Metab*. 2012;107(4):748–55. <https://doi.org/10.1016/j.ymgme.2012.10.011>.
- Galeano B, Klootwijk R, Manoli I, Sun M, Ciccone C, Darvish D, et al. Mutation in the key enzyme of sialic acid biosynthesis causes severe glomerular proteinuria and is rescued by *N*-acetylmannosamine. *J Clin Investig*. 2007;117(6):1585–94. <https://doi.org/10.1172/JCI30954>.
- Malicdan MC, Noguchi S, Hayashi YK, Nonaka I, Nishino I. Prophylactic treatment with sialic acid metabolites precludes the development of the myopathic phenotype in the DMRV-hIBM mouse model. *Nat Med*. 2009;15(6):690–5. <https://doi.org/10.1038/nm.1956>.
- Inker LA, Schmid CH, Tighiouart H, Eckfeldt JH, Feldman HI, Greene T, et al. Estimating glomerular filtration rate from serum creatinine and cystatin C. *N Engl J Med*. 2012;367(1):20–9. <https://doi.org/10.1056/NEJMoa1114248>.
- Shi Y, Xu X, Fang M, Zhang M, Li Y, Gillespie B, et al. Quantitative hydrophilic interaction chromatography-mass spectrometry analysis of *N*-acetylneuraminic acid and *N*-acetylmannosamine in

- human plasma. *J Chromatogr B Analyt Technol Biomed Life Sci.* 2015;1000:105–11. <https://doi.org/10.1016/j.jchromb.2015.07.018>.
21. Akaike H. Bayesian extension of the minimum AIC procedure of autoregressive model fitting. *Biometrika.* 1979;66:237–42. <https://doi.org/10.1093/biomet/66.2.237>.
  22. Dayneka NL, Garg V, Jusko WJ. Comparison of four basic models of indirect pharmacodynamic responses. *J Pharmacokinet Biopharm.* 1993;21(4):457–78. <https://doi.org/10.1007/BF01061691>.
  23. Bergstrand M, Hooker AC, Wallin JE, Karlsson MO. Prediction-corrected visual predictive checks for diagnosing nonlinear mixed-effects models. *AAPS J.* 2011;13(2):143–51. <https://doi.org/10.1208/s12248-011-9255-z>.
  24. Hinderlich S, Berger M, Keppler OT, Pawlita M, Reutter W. Biosynthesis of *N*-acetylneuraminic acid in cells lacking UDP-*N*-acetylglucosamine 2-epimerase/*N*-acetylmannosamine kinase. *Biol Chem.* 2001;382(2):291–7. <https://doi.org/10.1515/BC.2001.036>.